EVOLUTIONARILY STABLE DIFFUSIVE DISPERSAL

Alex Potapov and Ulrike E. Schlägel

Department of Mathematical and Statistical Sciences
University of Alberta
Edmonton AB T6G 2G1, Canada

Mark A. Lewis[1]

Department of Mathematical and Statistical Sciences
Department of Biological Sciences
University of Alberta
Edmonton AB T6G 2G1, Canada

Abstract. We use an evolutionary approach to find "most appropriate" dispersal models for ecological applications. From a random walk with locally or nonlocally defined transition probabilities we derive a family of diffusion equations. We assume a monotonic dependence of its diffusion coefficient on the local population fitness and search for a model within this class that can invade populations with other dispersal type from the same class but is not invadable itself. We propose an optimization technique using numerically obtained principal eigenvalue of the invasion problem and obtain two candidates for evolutionary stable dispersal strategy: Fokker-Planck equation with diffusion coefficient decreasing with fitness and Attractive Diffusion equation (Okubo and Levin, 2001) with diffusion coefficient increasing with fitness. For FP case the transition probabilities are defined by the departure point and for AD case by the destination point. We show that for the case of small spatial variability of the population growth rate both models are close to the model for ideal free distribution by Cantrell et al. (2008).

1. **Introduction.** Mathematical models for animal movement patterns have been the focus of much research [14, 19]. Typically the small-scale motion of an individual is described by random walk. Then, on a larger scale, the change in the expected population density of individuals is approximated by a partial differential equation. Depending on the details of the random walk, this equation may take several diffusion-type forms, ranging from classical diffusion equation, with a Fickian diffusive flux, to the Fokker-Planck (FP) equation, with a non-Fickian diffusive flux [2] (see also Section 2).

If the properties of the random walk are uniform in space, then the different formulations coincide to yield a simple diffusion equation with a constant diffusion coefficient, and there is no practical difference between the formulations. However, when the properties of the random walk vary according to spatial location, the different formulations can give very different outcomes. For example, the Fickian

[1]Corresponding author

diffusion model tends to equalize expected population density in different parts of the habitat. By way of contrast, the Fokker-Planck equation allows accumulation of the expected population density in spatial locations where motility (the FP equivalent of diffusion coefficient) is lower. The latter model appears biologically reasonable, and a number of authors have suggested that FP equation should be the more appropriate model for describing animal movement in spatially heterogeneous regions [19].

One approach to comparing and contrasting movement models is to employ an evolutionary approach, assessing which movement rules confer the highest fitness to the individuals undertaking them. For example, consider the competition of two interacting strains that have identical population dynamics but different dispersal mechanisms, described by different movement rules. If we allow the two strains to compete spatially and one strain outcompetes the other, then it is reasonable to conclude that the winner of the competitive interaction possesses a superior dispersal strategy. This approach has been proposed for determining the most advantageous value of a diffusion coefficient for a species in inhomogeneous but favorable habitat [6] and subsequently has been used to determine whether hypothesized dispersal mechanisms are evolutionarily stable strategies (ESS), e.g. [10].

To determine which dispersal mechanism is evolutionarily stable, it is necessary to define the dependence of the diffusion coefficient, or motility, on habitat characteristics. A commonly accepted measure of habitat quality is an individual's fitness, as measured by local per capita growth rate $\Phi = N^{-1}dN/dt$. Good quality habitat means high birth rates and low mortality and predation rates. Conversely, poor quality habitat lacks of the resources for high birth rates, and has higher mortality and predation rates. The per capita growth rate is typically density-dependent, often decreasing with population density. If the per capita growth rate is density-dependent then there is a feedback between habitat quality and population size. In this case, an evolutionarily stable dispersal strategy may give rise to an ideal free distribution (IFD), where individuals arrange themselves spatially so as to mirror the distribution of available resources [7, 8, 9, 11].

In the absence of dispersal, $\Phi = 0$ yields an equilibrium for N. If $\Phi > 0$ at a given location then it is a source, while if $\Phi < 0$ it is a sink. Fickian diffusion transfers individuals spatially, with a net flow from sources to sinks. At equilibrium, local fitnesses typically are nonzero. However, the spatially averaged population fitness $\langle \Phi N \rangle$ will equal zero, assuming no net immigration or emigration of individuals across the domain boundary. As we will show in this paper, non-Fickian diffusion allows for a more nuanced behavioral response to spatial variations in local fitness and need not give rise to a net flow from sources to sinks.

When modeling non-Fickian diffusion, it is reasonable to expect that the intensity of an individuals' movement will depend on local habitat quality. Predation risk also may stimulate individuals to move faster to escape the dangerous places or to "freeze" to become less visible to predators, e.g. [3]. One of the ways to model this type of behaviour may be to assume that parameters of the small-scale random walk depend on local fitness of individuals, which implies dependence of the diffusion coefficient or motility on local fitness.

In this paper we start with a random walk model where transition probabilities, from one location to the next, depending on local fitness values. Following [2], we consider three possibilities as to where the local values are measured: at the starting point of the transition, at the end point of the transition, or at some point in

between. In the first case, individuals choose to leave areas of low fitness (*repulsive transition* [14]). In the second case, individuals choose to move towards areas of higher fitness (*attractive transition*). We refer to the third case as the *neutral transition*, at least for the special case where measurement takes place at the midpoint between starting and end points. As we will show in Section 2, applying the standard random walk derivation of a diffusion-type equation to these cases leads to a family of diffusion-type equations which has the FP equation (via repulsive transitions), the Fickian diffusion equation (via neutral transitions) and the attractive dispersal (AD) equation (via attractive transitions) as special outcomes. We approach the question of finding an evolutionarily stable dispersal strategy as searching within this family of movement models for a model that cannot be invaded by any other model from the same family. We undertake this search using a hybrid analytical/numerical approach.

As described above, our family of dispersal models includes the simpler model of a constant diffusion coefficient in an environment with a spatially variable growth rate [6] as a special case. Dockery et al. [6] proved that the ESS for this simpler model is the minimum possible value, thus selecting against dispersal. However, our overall conclusions are different than those found in [6] because individuals in our model are not restricted to constant diffusion, but can choose more complex movement behaviours of the type described in the previous paragraph.

First, as we show in Section 3, it appears that the Fokker-Planck (FP) dispersal and attractive dispersal (AD) can invade any other dispersal type. In the case of a favourable but nonuniform habitat (the local intrinsic growth rate $r(x) > 0$ everywhere), as in [6], the ESS exhibits spatial variations of motility or diffusion coefficient reflecting the variations of local habitat quality with the mean value much higher than the minimum possible motility. The constant and minimum motility found in [6] did emerge as a local optimum, but not a global optimum, within our model family.

In case when habitat contains adverse parts ($r(x) < 0$), the result changes dramatically: the ESS yields a threshold dependence of motility on fitness: with the smallest possible motility in favourable locations ($r(x) > 0$) and the highest possible motility at the adverse locations ($r(x) < 0$) for FP dispersal and vice-versa for AD dispersal. Therefore, the environment, as described by the habitat type, determines the evolutionarily stable dispersal strategy, in agreement with ecological theories [12].

2. **Model development and analysis methods.** In this section we first consider several key assumptions of our model, and then formulate the full model.

2.1. **Random walk with intermediate decision point on a lattice and θ-dispersal diffusion-type term.** Consider an individual moving randomly on a discrete lattice with the spatial step δ and time step τ (Fig. 1). We assume that the probability of moving right, from x to $x + \delta$, depends on coordinate at some intermediate point $x + \theta\delta$, $0 \leq \theta \leq 1$; similarly the probability of moving left depends on coordinate at the point $x - \theta\delta$. The probabilities at each time step of moving right R, left L, and staying put S depend on conditions at the coordinate. Using a standard approach (e.g. [14, 19], see Appendix for details) one can derive equation governing the probability distribution for the individual $u(x, t)$ in the limit $\delta, \tau \to 0$:

$$\frac{\partial u}{\partial t} = \frac{\partial}{\partial x}\left(-c(x)u + (1 - 2\theta)D'(x)u + D(x)\frac{\partial u}{\partial x}\right),$$
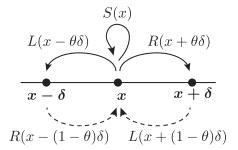
FIGURE 1. Scheme of random walk with decision depending on different locations.

where

$$c\left(x\right) = \lim_{\delta,\tau \to 0} \frac{\delta}{\tau}\left(R\left(x\right) - L\left(x\right)\right)$$

is the advection speed and

$$D\left(x\right) = \lim_{\delta,\tau \to 0} \frac{\delta^2}{2\tau}\left(R\left(x\right) + L\left(x\right)\right),$$

is *diffusion coefficient*. We assume that both limits exist. For the sake of focusing on the motility component of the random walk we ignore the bias term and assume that the advection $c\left(x\right) = 0$. For notational brevity we denote $u_x = \partial u/\partial x$. Assuming also that for $\theta > 0.5$, $D\left(x\right) \neq 0$, the equation can be written in divergence form,

$$u_t = \left(D^{2\theta}\left(D^{1-2\theta}u\right)_x\right)_x. \tag{1}$$

From this expression it follows that the flux is $J = -D^{2\theta}\left(D^{1-2\theta}u\right)_x$.

Now we can see that the values $\theta = 0, 0.5, 1$ correspond to known cases [19, 14]:

- $\theta = 0$: $u_t = \left(Du\right)_{xx}$, Fokker-Planck equation arising from a *repulsive transition* according to [14] classification;
- $\theta = 0.5$: $u_t = \left(Du_x\right)_x$, Fickian diffusion equation arising from a *neutral transition*;
- $\theta = 1$: $u_t = \left(D^2\left(u/D\right)_x\right)_x$, attractive dispersal (AD) equation arising from an *attractive transition*.

Equation (1) includes all three cases into a one-parameter family of dispersal models, which we shall call the θ-*diffusion equation*. The parameter θ reflects the way individuals make decision, and hence it may be a trait of individuals and subject to mutation and selection. We cannot exclude existence of strategy where dispersal should be described by (1) with a range of different θ values. Potentially this situation could be quite complicated, and within one strain there could be a mixture of individuals dispersing according to different rules. However, we shall not consider such generalizations here, and will focus on pure strategies where θ attains a single value.

2.2. **Local population dynamics and full model.** We assume that the modeled population can be described by an expected population density $u\left(x,t\right)$. We assume that fitness of per capita reproduction and mortality can be described by a linear function of u,

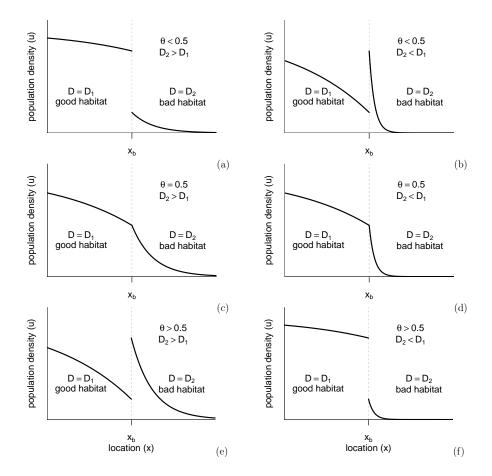$$\Phi\left(x,u\right) = r\left(x\right) - m\left(x\right)u, \tag{2}$$

FIGURE 2. Examples of behaviour of $u(x,t)$ at the interface between habitats with positive (good habitat) and negative (bad habitat) intrinsic growth rates for different D_1/D_2 and θ. For $\theta \neq 0.5$ the interface appears to be "active", it creates additional flow of individuals from one side to the other. In some cases it is favourable for the species ("pumping" from a bad habitat into a good one, panels a and f), in other cases it is adverse ("pumping" from a good habitat into a bad one, panels b and e). See Section 2.2 and Appendix for the details.

where r is the intrinsic growth rate and m is the density-dependent reduction in growth rate. If the local birth rate for a rare population is greater than mortality then $r(x) > 0$. If not then $r(x) \leq 0$. The term $m(x)u$ describes the density-dependent increase in mortality or decrease in birth rate, and we assume $m(x) > 0$. In numerical calculations presented in Section 3 we used a spatially varying growth rate

$$r(x) = r_{\min} + A \sin^2 (2\pi x/L), \qquad m = 1, \tag{3}$$

with $r_{\min} + A > 0$ so as to prevent the population from going extinct.

The full population model that we consider is

$$u_t = \left(D^{2\theta}\left(D^{1-2\theta}u\right)_x\right)_x + \Phi\left(x, u\right)u, \qquad 0 < x < L, \quad t > 0, \quad u\left(0\right) = u_0\left(x\right).$$

$$(4)$$

For simplicity we assume zero flux boundary conditions, which for $D > 0$ are

$$\left(D^{1-2\theta}u\right)_x\big|_{x=0,L} = 0. \tag{5}$$

When the diffusion coefficient is spatially uniform, the diffusion equation ceases to depend on θ: in all cases we have the equation $u_t = Du_{xx} + \Phi\left(x, u\right)u$. The interpretation is clear: if there is no spatial dependence, all types of decision making give the same outcome. However, *any* spatial dependence changes the situation and the choice of model may strongly influence the properties of the solution.

To see this we consider a simple example. Assume that the species' habitat consists of two subdomains. Within subdomain 1 the diffusion coefficient is spatially uniform and equal to D_1. Within subdomain 2 it is also spatially uniform, but equals $D_2 \neq D_1$. How does the solution look in the vicinity of the boundary between the domains? The properties of the solution can be derived from the requirement of continuity and differentiability of the terms in the equation. Therefore, both terms $D^{1-2\theta}u$ and $D^{2\theta}\left(D^{1-2\theta}u\right)_x$ should be continuous at the boundary, that is their values to the right and to the left of the boundary should coincide. We denote the value of u and u_x near the boundary within each domain as u_1, u_2, u_{1x}, u_{2x}. Also note that within each domain, due to uniformness of D, $D^{2\theta}\left(D^{1-2\theta}u\right)_x = Du_x$. Continuity means that $D_1^{1-2\theta}u_1 = D_2^{1-2\theta}u_2$ and $D_1u_{1x} = D_2u_{2x}$. They can be written as

$$\frac{u_2}{u_1} = \left(\frac{D_1}{D_2}\right)^{1-2\theta}, \qquad \frac{u_{2x}}{u_{1x}} = \frac{D_1}{D_2}. \tag{6}$$

Therefore, near the boundary separating D_1 and D_2 there always is a change of slope of the $u\left(x\right)$ profile. In case of $\theta \neq 0.5$ there should also be a jump in u values, that is the profile $u\left(x\right)$ should be discontinuous at the boundary, see Fig. 2 and Appendix.

The discontinuity means that the boundary between the two values of diffusion coefficient is partially attractive from one side and partially reflective from the other. This feature may help individuals to stay in better habitat with $r > 0$, Fig. 2a,f, or, on the contrary, push them out to worse one with $r < 0$, Fig. 2b,e. For $\theta < 0.5$, e.g. in case of FP equation, individuals concentrate in the domain of smaller D, while for $\theta > 0.5$ they are attracted to greater D values. Assuming that individuals tend to concentrate in better habitat (IFD-like behaviour), the first case corresponds to a species where individuals move only slightly in good conditions, but try to actively escape from adverse ones, like fish (Fig. 2a). The second case corresponds to a species which is in a constant motion in good conditions, e.g. looking for food, but is almost stationary in adverse ones, e.g. to be less visible to predators, like some bottom crawling insects do (Fig. 2f).

A detailed analysis of discontinuities at a boundary for a different model of random walk, with equal right or left transition probabilities but different right and left step length can be found in [15].

2.3. **Diffusion coefficient and fitness.** We assume that individuals may move differently when their local fitness Φ changes, see e.g. [5, 1]. For example, when habitat is good, that is there are enough resources and predation is low, individuals may stay put with greater probability. On the other hand, when habitat is adverse,

they may have greater probability to change their location. At the same time they cannot stop moving totally, and there is a natural limit to their motility. Therefore we assume that D is always nonzero and bounded

$$0 < D_{\min} \le D(\Phi) \le D_{\max} < \infty.$$

A second assumption is that $D(\Phi)$ does not have maxima or minima. It should take one of three forms: a decreasing function of fitness, a constant, or an increasing function of fitness. When we implement the model numerically we approximate this relationship by a sigmoid curve

$$D(\Phi) = S(\Phi) = D_{\min} + \frac{D_{\max} - D_{\min}}{1 + \exp(a - b\Phi)}. \tag{7}$$

This expression approaches a constant diffusion coefficient if $b/a \to 0$ (neutral transition with respect to fitness). It is a decreasing function (decreased motility under higher fitness conditions) if $b < 0$ and an increasing one (increased motility under higher fitness conditions) if $b > 0$. Proper adjustment of a and b can give both a smooth gradually changing function (b/a small) or a step-like dependence with a threshold (b/a large). This appears to be sufficient for a qualitative study of the problem.

2.4. **Temporal variations of diffusion coefficient and individuals' decision making.** When D is a function of local fitness, and the local fitness changes with time, there is a possibility of an instantaneous feedback loop: the redistribution of individuals changes fitness, and the changes in fitness instantly cause new redistribution of individuals. This can lead to development of an instability, either in the model or in its discrete numerical approximation. Biologically we also expect that the assumption of an instantaneous response to local conditions will not hold. Specifically, there will be a slower time scale over which behaviour adjusts to changing environmental conditions. We allowed a characteristic relaxation time scale γ^{-1} for behavioural changes to occur, and instead of employing (7) directly, we introduced $D(x, t)$ satisfying

$$D_t = \gamma(S(\Phi(x, u)) - D), \tag{8}$$

where γ is the relaxation rate, which is inversely proportional to time needed for individuals to assess the current situation. This equation adds a low-pass filter, and prevents short-time instabilities. In numerical calculations we chose γ such that the model eventually converged to a steady state. For $\gamma \to \infty$ one obtains (7).

2.5. **Searching for the evolutionarily stable strategy.** The standard test for dispersal strategy being an ESS [10] involves bringing the system (4) to the steady state $u_*(x)$ so that

$$\left(D^{2\theta}\left(D^{1-2\theta}u_*\right)_x\right)_x + \Phi(x, u_*)u_* = 0, \tag{9}$$

$$0 < x < L, \quad \left(D^{1-2\theta}u_*\right)_x\big|_{x=0,L} = 0.$$

and then introducing a small amount of a probe competing species $v(x, t)$ obeying the same local population dynamics $\Phi(u + v, x)v$, but having different $\hat{D}(\Phi)$ and $\hat{\theta}$. The joint dynamics of the two species is then described by system

$$u_t = \left(D^{2\theta}\left(D^{1-2\theta}u\right)_x\right)_x + \Phi(x, u + v)u, \tag{10}$$

$$v_t = \left(\hat{D}^{2\hat{\theta}}\left(\hat{D}^{1-2\hat{\theta}}v\right)_x\right)_x + \Phi(x, u + v)v, \tag{11}$$

and boundary conditions (5) for both u and v. If $\|v\| \ll \|u\|$, then $u + v \approx u \approx u_*$, $\Phi(x, u + v) \approx \Phi(x, u_*)$, and system (10), (11) splits into two: equation (4) for u and equation for v:

$$v_t = \left(\hat{D}^{2\hat{\theta}} \left(\hat{D}^{1-2\hat{\theta}} v \right)_x \right)_x + \Phi(x, u_*)\, v. \tag{12}$$

The invader diffusion coefficient, $\hat{D}$, is calculated as as $\hat{D} = \hat{S}(\Phi(x, u_*))$, see (7). Here $\hat{S}$ denotes S being calculated for different values of $a = \hat{a}$ and $b = \hat{b}$. Now (12) is a linear equation for v, and growth or decay of v is described by the eigenvalue problem

$$\left(\hat{D}^{2\hat{\theta}} \left(\hat{D}^{1-2\hat{\theta}} w \right)_x \right)_x + \Phi(x, u_*)\, w = \lambda w, \qquad \left(\hat{D}^{1-2\hat{\theta}} w \right)_x \Big|_{x=0,L} = 0, \tag{13}$$

which is equivalent to

$$\hat{D}^{1-2\hat{\theta}} \left(\hat{D}^{2\hat{\theta}} \psi_x \right)_x + \Phi(x, u_*)\, \psi = \lambda \psi, \qquad \psi_x|_{x=0,L} = 0, \qquad \psi = \hat{D}^{1-2\hat{\theta}} w \tag{14}$$

since $D \geq D_{\min} > 0$. According to the version of Krein-Rutman theorem by Cantrell and Cosner [4], the principal eigenvalue of (13), (14) $\lambda_{\max}$ is real and the associated eigenvector w can be chosen to be positive. By definition of the principal eigenvalue, all other eigenvalues λ satisfy $\mathrm{Re}\lambda < \lambda_{\max}$, see e.g. [13] for a similar problem.

As described above, we consider the case when D depends on two parameters, a and b (7). The steady state $u_*(x)$ to equation (4) depends on parameters a, b, and θ, and this steady state appears in the eigenvalue equation for the dynamics of the invader (13). Thus we denote the dependence of the maximum eigenvalue on these parameters by writing $\lambda_{\max}\left(\hat{a}, \hat{b}, \hat{\theta} | a, b, \theta\right)$. Here we assume that values for the parameters are on the closed intervals $a_{\min} \leq a, \hat{a} \leq a_{\max}$, $b_{\min} \leq b, \hat{b} \leq b_{\max}$, and $0 \leq \theta, \hat{\theta} \leq 1$ where $a_{\min}, b_{\min} < 0$ and $a_{\max}, b_{\max} > 0$.

If $\lambda_{\max}\left(\hat{a}, \hat{b}, \hat{\theta} | a, b, \theta\right) > 0$, then the new species can invade the population and the original dispersal strategy a, b, θ is not an ESS. If, on the other hand, the maximum over all possible dispersal strategies

$$\max_{\hat{a}, \hat{b}, \hat{\theta}} \lambda_{\max}\left(\hat{a}, \hat{b}, \hat{\theta} | a, b, \theta\right) = 0, \tag{15}$$

then the dispersal strategy, a, b, θ, is an ESS. Note that this maximum cannot be negative because, for $\hat{a} = a$, $\hat{b} = b$, $\hat{\theta} = \theta$, (13) always has the zero eigenvalue corresponding to $w = u_*$ and therefore $\max_{\hat{a}, \hat{b}, \hat{\theta}} \lambda_{\max}\left(\hat{a}, \hat{b}, \hat{\theta} | a, b, \theta\right) \geq 0$. Therefore (15) becomes optimization problem over three *resident* parameters: a, b, θ, where each parameter is taken to be on the closed intervals described above, and three *invader* parameters $\hat{a}, \hat{b}, \hat{\theta}$, over which the maximization occurs. These invader parameters are also taken to be on the closed intervals described above. The weaker case where (15) is satisfied for $\hat{a}, \hat{b}, \hat{\theta}$ in some local neighborhood of a, b, θ is referred to as a *local* ESS. In general, the condition (15) for an ESS can occur when the parameters a, b and θ are in the interior of the closed parameter sets (*interior* ESS) or can occur when the parameters are on a boundary of the closed parameter sets (*boundary* ESS).

As a reminder, the behavioural interpretations of the parameters are given: θ represents the degree to which movement decisions are made on purely local conditions ($\theta = 0$) or nonlocal conditions ($\theta = 1$), the sign of b represents attractivity/repulsion

in the random walk towards regions of higher fitness and b/a represents the sensitivity of the random walk to fitness (see (7)). As described earlier, the case $b < 0$ and $\theta = 0$ describes repulsion from low fitness regions whereas the case $b > 0$ and $\theta = 1$ describes attraction towards high fitness regions.

Numerically it is most efficient not to solve the full eigenvalue problem (13), but to use the technique resembling calculation of Lyapunov exponents. We set an initial guess, say, $v = u_*$, and then solve (12), periodically renormalizing $v \to v/\|v\|$. After long enough time period t_C the spatial profile of $v(x, t_C)$ converges to the eigenfunction $w_1(x)$ corresponding to the largest eigenvalue λ_{LE} with the required accuracy ϵ_w, because $\lambda_{\max}$ is strictly greater than the real part of all other eigenvalues [4]. Then, since $\lambda_{\max}$ is real, $v(x, t_C + T) = \|v(x, t_C)\| \cdot w_{\max}(x) \cdot \exp(\lambda_{\max} T)$, $T > 0$, and hence

$$\lambda_{\max} \approx T^{-1} \log\left(\|v(x, t_C + T)\| / \|v(x, t_C)\|\right). \tag{16}$$

In numerical calculations below $\epsilon_w = 10^{-6}$ and $T = 10$.

Our initial numerical investigations showed that local evolutionarily stable strategies were found on the parameter boundaries (local boundary ESSs). In particular, they gave either $b = b_{\min}$ and $\theta = 0$ (repulsive transition) or $b = b_{\max}$ and $\theta = 1$ (attractive transition). These local boundary ESSs remained on the boundary even as $b_{\min}$ was lowered and $b_{\max}$ was raised. Thus, to understand this phenomenon we gradually varied b and generated pairwise invasibility plots as a function of b. Specificially, we first set b, at various values, b_i that were incremented between $b_{\min}$ and $b_{\max}$. Then, for each value b_i we applied the following numerical algorithm.

1. Set an initial guess for the parameters a_0, θ_0.
2. Find the steady state solution $u_*(x|a_k, b_i, \theta_k)$.
3. Find a_{k+1}, θ_{k+1} that give the greatest value of $\lambda_{\max}(a_{k+1}, b_i, \theta_{k+1}|a_k, b_i, \theta_k)$. For this step we use the combination of random search and optimization routine optim from R [17]. First we do 100 steps of hide-and-seek algorithm [18, 16], then use its best result as initial guess for optim.
4. If $|a_{k+1} - a_k| + |\theta_{k+1} - \theta_k| > \epsilon_{\text{tol}}$, return to step 2.

In our implementation of the numerical algorithm we chose $\epsilon_{\text{tol}} = 10^{-6}$.

If this algorithm converges and in step 3 the global maximum is found, then the species with resulting dispersal cannot be invaded by any other species from the same dispersal class, and hence the ESS is found within a class of diffusion coefficients with fixed fitness attractivity b_i. This ESS is described by a value of $a = a_i$ and $\theta = \theta_i$ associated with the fixed fitness attractivity b_i, and is denoted by $\text{ESS}(b_i)$. The parameters $a = a_i$ and $b = b_i$ then determine the functional relationship between motility D and fitness $\phi(x, u)$ described in (7). Substitution into (9) along with parameter $\theta = \theta_i$ then yields a steady state u_* associated with $\text{ESS}(b_i)$.

We then chose the ESS (a_i, b_i, θ_i), as calculated for the fixed b_i, to be the *resident b-strategy*, and evaluated the maximum eigenvalue associated with other levels of attractivity b_j, that is estimated $\lambda_{\max}(a_j, b_j, \theta_j|a_i, b_i, \theta_i)$ in (16) to see if any other b-strategy could invade. This was used to generate pairwise invasibility plots based on the level of attraction/repulsion of the random walk to fitness levels, as measured by the parameter b.

Our initial investigations used a more complex version of this algorithm, where b was also allowed to vary, as well as a and θ. However, the hierarchical approach to

Table 1. Model parameters

Parameter or term	Meaning and reference	Values in calculations
$r(x)$	intrinsic growth rate, (2), (3)	$r_{\min} + A\sin^2(2\pi x/L)$
$m(x)$	density-dependent mortality, (2)	1
$r_{\min}$	minimum growth rate, (3)	-2, 0, 1
A	magnitude of growth rate change, (3)	3, 1, 0.1
θ	type of random walk producing diffusion, (1)	$0 \le \theta \le 1$
$D_{\min}$	minimum diffusion coefficient $D(\Phi)$, see (7)	0.1
$D_{\max}$	maximum diffusion coefficient $D(\Phi)$, see (7)	1
a	determines $D(0)$, see (7)	varies
b	determines maximum steepness of $D(\Phi)$, see (7)	varies

ESS analysis, where b is first fixed for the ESS analysis, and then was systematically varied, generated results that were more robust and straightforward to interpret.

3. **Results.** In numerical calculations presented here, the ranges of dispersal parameters we used were $D_{\min} = 0.1$, $D_{\max} = 1$, $a_{\min} = -30$, $a_{\max} = 30$, $b_{\min} = -20$, $b_{\max} = 20$, $\theta_{\min} = 0$, and $\theta_{\max} = 1$, see Table 1. In calculations for the steady state, the initial value was $\gamma = 5$. If convergence to the steady state was not reached during first 100 time units, then γ was divided by 2. After each 100 time units γ was decreased again until convergence to the steady state was reached. Fitness did not change during invasibiliy tests, so there was no need in the relaxation calculations of D. The parameters describing the spatial environment were as follows: the domain length $L = 10$ and in the relation for the local growth rate (3) a variety of values for $r_{\min}$ (negative, zero and positive values) and A (positive values of different magnitude) was used, see Table 1. The fitness function (2) used $r(x)$ as described by equation (3) and used density-dependent mortality $m(x) = 1$.

For fixed b, the dispersal strategy optimization algorithm typically converged in about 10 iterations. The type of the resulting ESS(b) dispersal strategy depended on b. Figure 3 shows the type of the ESS(b) strategy for each habitat in our simulations.

If $|b|$ was small, then the dispersal strategy converged to $D \approx D_{\min}$, with b/a close to zero in equation (7) (see Figure 3). The solid line shows maximum attained value of the diffusion coefficient over all possible values of x, $\max D(\Phi)$. For the dispersal strategy with constant diffusion coefficient $D = D_{\min}$, $\max_x D(\Phi) = D_{\min}$. This corresponds to the flat part in Figure 3 with fitness attractivity values b near $b = 0$. If b was larger and negative, the algorithm always converged to the case $\theta = 0$, that is to the Fokker-Planck (FP) equation (repulsive transition). Alternatively, if b was larger and positive, the algorithm always converged to the case $\theta = 1$, that is to the AD equation (attractive transition). Both the repulsive transition and attractive transition dispersal give higher values of $\max D(\Phi)$. Circles in Figure 3 show the value of θ, for the left part of the plot ESS always corresponds to FP or repulsive transition dispersal with $\theta = 0$, the right part corresponds to AD dispersal with $\theta = 1$. The portion with $D = D_{\min}$ gives a dispersal strategy D that is constant and independent of fitness Φ. Hence it is also independent of spatial location. Thus
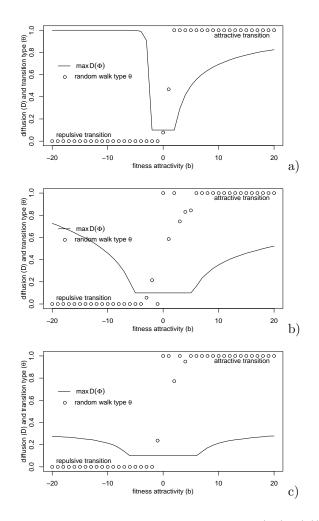
FIGURE 3. Maximum diffusion coefficient $\max_x D\left(\Phi\left(u_*\left(x\right)\right)\right)$ and the random walk type θ for numerically obtained ESS(b) dispersal for fitness attractivity $b = -20, -19, \ldots, 20$. The types of habitat are determined by the local intrinsic growth rate $r(x) = r_{\min} + A\sin(2\pi x/L)^2$ (3): a) $r_{\min} = -2$, $A = 3$; b) $r_{\min} = 0$, $A = 1$; c) $r_{\min} = 1$, $A = 0.1$. In each panel there are three parts corresponding to three different dispersal strategies: big negative b correspond to FP or repulsive transition dispersal ($\theta = 0$), the middle part around $b = 0$ corresponds to constant $D = D_{\min} = 0.1$ (for constant D the equation (4) does not depend on θ and numerically obtained values vary), big positive b correspond to attractive transition (AD) dispersal ($\theta = 1$).

the equation (4) ceases to depend on θ, so optimization can yield various θ values between 0 and 1 (Figure 3). This simple diffusion strategy is independent of the value for θ (see equation (4)). As can be seen from Figure 3, the calculated θ values are highly variable when $D \approx D_{\min}$.

Therefore, ESS(b) gives three potential global ESS candidates: the minimum constant diffusion equation, the FP equation and the AD equation. They differ in sensitivity to the local fitness: no sensitivity, negative sensitivity with $\theta = 0$, and positive sensitivity with $\theta = 1$. Actually, this could be expected from the profiles in Fig. 2a,f.

The corresponding steady state profiles $u_*(x)$ and dispersal coefficients $D(\Phi(x))$ are shown in Figure 4 for the FP case ($b = -20$) and in Figure 5 for the AD case ($b = 20$). Notice how $D(\Phi(x))$ correlates negatively with $r(x)$ for the FP case and positively with $r(x)$ for the AD case. Both figures show the case of a mixture of good and strongly adverse habitat (panel a, $A = 3$, $r_{\min} = -2$), a good habitat of strongly varied quality (panel b, $A = 1$, $r_{\min} = 0$), and a good habitat with slightly varied quality (panel c, $A = 0.1$, $r_{\min} = 1$). In panel a we see strong variations of diffusion coefficient $D(x)$ with respect to the habitat quality, while in panel c only slight variations. The same is true about the variation of the local fitness. The relationship between D and Φ given in the three profiles in Fig.4 and Fig.5, is shown in Figure 6, panels a and b respectively.

The next step was to test mutual invasibility of the obtained ESS(b) strategies. Although an exhaustive study would require an analytical technique, our approach was to employ a numerical investigation. Here, we calculated $\lambda_{\max}(a_j, b_j, \theta_j | a_i, b_i, \theta_i)$ for each pair of b_i, b_j numerically. The results for mutual invasibility are presented in Figure 7, panels a, b, and c correspond to the same habitat types as in Figures 3, 4, and 5. Each panel shows b for the resident species along x-axis and b for the invader along y-axis. Filled black circles on the plot shows a situation when the invader can invade ($\lambda_{\max} > 0$); empty circles correspond to a situation when invasion fails ($\lambda_{\max} < 0$); finally the grey circles corresponds to a neutral situation ($\lambda_{\max} = 0$), when the invader neither grows nor goes extinct, or when it is impossible to distinguish the situation numerically ($|\lambda_{\max}| \leq 10^{-6}$). The results depend on the habitat and the type of the pair resident–invader and can be summarized as follows.

1. Both repulsive transition (FP) dispersal and attractive transition (AD) dispersal strategies can invade the dispersal with constant $D = D_{\min}$, while the latter can not invade repulsive transition or attractive transition dispersal with $|b|$ exceeding a certain threshold, depending on the habitat type.
2. When the invader and resident are both of the same type FP or AD, then the strategy corresponding to the greater $|b|$ can invade the strategy with the smaller $|b|$.
3. In good habitat FP-dispersal can invade AD-dispersal with smaller $|b|$, and vice-versa (panels b and c in Fig. 7).
4. In a combination of good and bad habitat (panel a in Fig. 7) AD-dispersal typically can invade FP-dispersal, but FP-dispersal can only invade AD-dispersal with small b.

When we first obtained the result that $D = D_{\min}$ is not an ESS, we thoroughly tested it to exclude numerical error. The examples of solutions shown in Figs. 4c and 5c satisfy the conditions of the theorem in [6], however D is slightly oscillating near the mean value, with a mean value of approximately $3D_{\min}$, which is quite far from $D_{\min}$. We tested each obtained ESS profile to invasibility by a species with $D = D_{\min}$ (the value θ in this case does not matter) by calculating $\lambda_{\max}$ (16). In all cases $\lambda_{\max} < 0$, but small, $\approx -10^{-3}$. For a few profiles we made numerical calculations of explicit competition of the two species in the system (10), (11) starting with
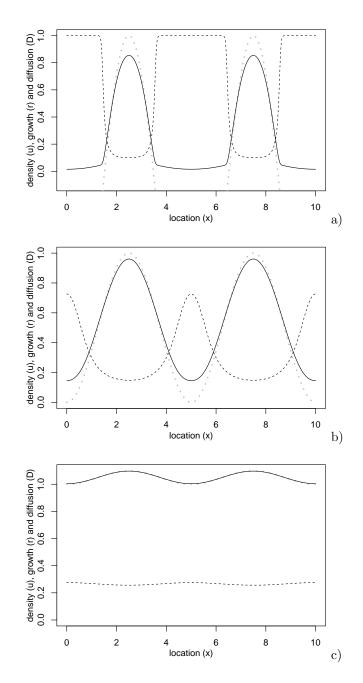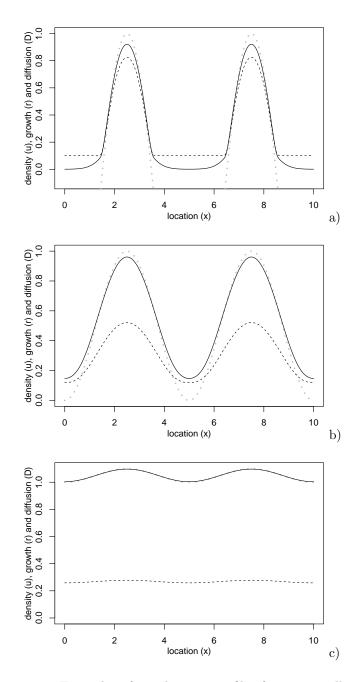
FIGURE 4. Examples of steady-state profiles for numerically ob-tained ESS(b) dispersal for $b = -20$. Solid line $u_*(x)$, dashed line $D(\Phi(x))$, gray dotted line $r(x)$. In all shown cases iterations con-verged to $\theta = 0$ or Fokker-Planck (FP) dispersal. Parameter a and the resulting motility depend on $r(x)$, that is on the properties of the habitat. a) $r_{\min} = -2$, $A = 3$, $a = 3.34$; b) $r_{\min} = 0$, $A = 1$, $a = 2.08$; c) $r_{\min} = 1$, $A = 0.1$, $a = 1.49$.

FIGURE 5. Examples of steady-state profiles for numerically obtained ESS(b) dispersal for $b = 20$. Solid line $u_*(x)$, dashed line $D(\Phi(x))$, gray dotted line $r(x)$. In all shown cases iterations converged to $\theta = 1$ or attractive transition (AD-dispersal). Parameter a and the resulting motility depend on $r(x) = r_{\min} + A\sin(2\pi x/L)^2$, that is on the properties of the habitat. a) $r_{\min} = -2$, $A = 3$, $a = 0.16$; b) $r_{\min} = 0$, $A = 1$, $a = 0.92$; c) $r_{\min} = 1$, $A = 0.1$, $a = 1.47$.
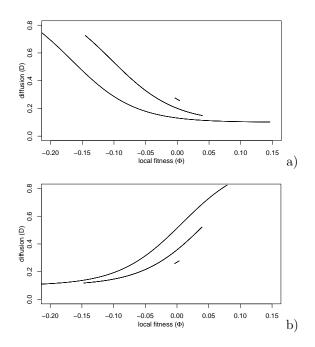
FIGURE 6. Numerically obtained $D(\Phi)$ for the three profiles in Fig.4 (panel a) and Fig.5 (panel b). In panel a lower to upper curves correspond to Fig.4a,b,c respectively. In panel b upper to lower curves correspond to Fig.5a,b,c. Shown only the part of the plot near $\Phi = 0$ and only for those values of Φ, which arise in the actual solution.

identical initial conditions for each species: $u(x,0) = v(x,0) = 0.5\, r(x)/m(x)$. The competitive outcomes took a long time to simulate (approximately 10^5 time units) but eventually the species with fitness-driven dispersal drove the competitor with $D = D_{\min}$ to extinction.

4. **Discussion.** Our numerical investigations lead us to several general insights, given below.

Connection between global ESS dispersal strategies. There appear to be two candidates for the "global ESS dispersal strategy", that is the dispersal strategy that can invade any other dispersal strategy within the same class: Fokker-Planck (repulsive transition) dispersal ($\theta = 0$) with decreasing $D(\Phi)$ and Attractive Dispersal (attractive transition) ($\theta = 1$) with increasing $D(\Phi)$. Both of these can be written in similar form,

$$u_t = (Du_x)_x \pm (uD_x)_x + \Phi(x,u)\, u. \tag{17}$$

Here the '+' sign corresponds to $\theta = 0$ and '−' sign to $\theta = 1$. Another similarity is in the fact that both equations can generate spatially nonuniform profiles in case of spatially nonuniform diffusion coefficient. In the absence of growth term and in case of zero flux boundary conditions the FP equation has the steady state $u_* \propto D^{-1}$ and, because of this in particular, P. Turchin suggested that FP equation may be most suitable to ecological movement with complex behavioural strategies [19]. As
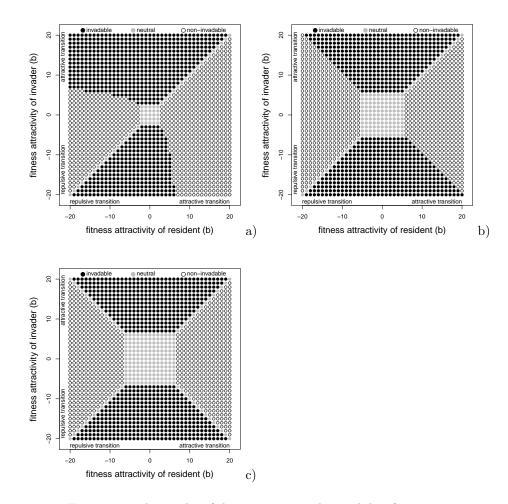
FIGURE 7. The results of the test on mutual invasibility for numerically obtained ESS(b) dispersal for fitness attractivity parameter $b = -20, -19, ..., 20$. x-axis shows b for the resident species, y-axis shows b for the invader. Black circle denotes successful invasion ($\lambda_{\max} > 0$), white dot denotes failed invasion ($\lambda_{\max} < 0$), gray dot denotes coexistence or neutral case ($\lambda_1 = 0$) or situations numerically indistinguishable from it ($|\lambda_{\max}| < 10^{-6}$). a) $r_{\min} = -2$, $A = 3$; b) $r_{\min} = 0$, $A = 1$; c) $r_{\min} = 1$, $A = 0.1$. The gray square in the centre corresponds to constant $D = D_{\min} = 0.1$ dispersal, there is the same dispersal strategy for a range of b values near zero.

we have shown here, the AD equation has a similar property; its solution under the same conditions is $u_* \propto D$, and it appears that it may be as good in ecological applications as the FP equation. Moreover, if we substitute $D = D(\Phi)$, then both equations turn into a single equation,

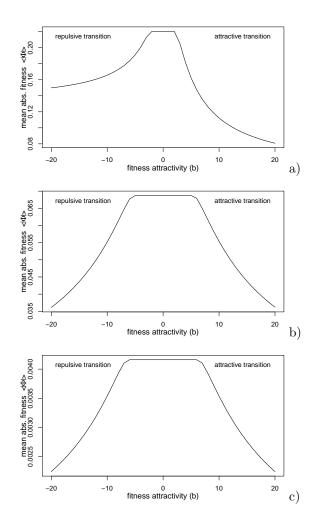$$u_t = (Du_x)_x - (u\,|D_\Phi|\,\Phi_x)_x + \Phi(x, u)\,u, \tag{18}$$

FIGURE 8. Examples of $\langle |\Phi| \rangle_*$ plots (19) for numerically obtained ESS(b) dispersal for the steepness parameter $b = -20, -19, \ldots, 20$. a) $r_{\min} = -2$, $A = 3$; b) $r_{\min} = 0$, $A = 1$; c) $r_{\min} = 1$, $A = 0.1$. The smaller $\langle |\Phi| \rangle_*$ is, the closer is the profile to ideal free distribution (IFD), for which $\langle |\Phi| \rangle_* = 0$. Comparison with Fig. 7 allows us to conjecture that dispersal strategies with smaller $\langle |\Phi| \rangle_*$ can invade those with greater $\langle |\Phi| \rangle_*$.

since we have $D_\Phi < 0$ for FP case and $D_\Phi > 0$ for AD case. Therefore, in the case of fitness-dependent ESS dispersal, both equations describe Fickian diffusion augmented with taxis along the gradient of local fitness. However, in spite of very similar mathematical form, the FP and AD equations correspond to very different behavioural strategies, both of which appear to be competitive. Profiles of $u_*(x)$ in Figs. 4a and 5a also have some difference: in AD case the values of $u_*(x)$ in adverse habitat parts are smaller, which gives less intensive population sink.

Boundary ESS solutions. For both repulsive and attractive transition dispersal it appears that the greater is the steepness of the $D(\phi)$ profile, that is the

greater is absolute value of fitness attractivity $|b|$, the more competitive the dispersal strategy becomes. In our investigations, where b was constrained to lie between $b_{\min}$ and $b_{\max}$, this led to boundary ESS solutions. Therefore it is natural to assume that the true optimum in the unconstrained case is $|b| \to \infty$. That is, there is a threshold fitness Φ_0, such that for FP case $D = D_{\max}$ for $\Phi < \Phi_0$ and $D = D_{\min}$ for $\Phi > \Phi_0$ (for AD case inequalities are the opposite). Mathematically this case is complex to analyze, both analytically and numerically. However, biologically, at the level of individual, it looks quite simple: just involving switching between two types of behaviour, active and passive, due to some fitness-related cue.

There may, however, be a biologically-related limits on behaviour, giving rise to $b_{\max}$ and $b_{\min}$, due to the functioning of the behaviour-switching cues. In this case, the boundary ESS value is determined by the biological limits to behavioural switching.

Connecting to models for the IFD. The result of Dockery et al. in [6], that give constant $D = D_{\min}$ as the ESS when diffusion is restricted to being constant in space, holds here also in the case when the species effectively cannot use the dependence of D on fitness, that is $|b|$ is restricted to small values. Then it appears optimal to abandon the dependence of movement on fitness totally and to disperse at the minimum rate (Fig. 3). Moreover, this strategy seems to remain valid even in case when $r(x)$ may attain zero or negative values as well (Fig. 3a,b). That is, it appears to remain valid in a more general case than proven in [6]. However, this strategy may be easily outcompeted by a species that has learned fitness-dependent dispersal with large enough $|b|$.

The deviations of the diffusion coefficient from a constant in Figures 4c and 5c are very small, and the profile looks almost constant. Then the question arises as to why $D = D_{\min}$ fails to be an optimum. Figure 6 suggests an approximate consideration of this case. One can see that Φ for the case $r_{\min} = 1$, $A = 0.1$ changes within a very small range of values, such that instead of a full sigmoid "step" in $D(\Phi)$ we see only a small piece close to a straight line. Therefore, we can use an approximation $D(\Phi) \approx D(0) + \beta\Phi$ with $\beta < 0$ for FP dispersal and $\beta > 0$ for AD one. Then $D_\Phi = \beta$ and (18) in both FP and AD cases takes the form

$$u_t = (Du_x)_x - |\beta|(u\Phi_x)_x + \Phi(x, u)u,$$

and has a strong resemblance with the model for Ideal Free Distribution proposed by Cantrell et al. [5], which uses advection along the gradient of fitness. Therefore, it is natural to suggest that FP or AD dispersals are evolutionarily stable because they provide a spatial distribution of individuals closer to IFD than the model with just $D = D_{\min}$.

Understanding deviations away from the IDF. There is a possibility that closeness to IFD could be an explanation for our ESS results: the closer the resulting population density profile to IFD, the more competitive the dispersal strategy is. The exact IFD at equilibrium $u_*(x)$ corresponds to $\Phi = 0$ at the domains where $r(x) > 0$ (maximum possible population density) and $u_* = 0$ where $r(x) \le 0$; see [5] for an example. Therefore, the product $\Phi(u_*)u_*$ at equilibrium IFD is zero everywhere. If we characterize the deviation away from the state $\Phi u_* = 0$ as a mean value of $|\Phi|$ weighted by $u_*(x)$, then, at the exact IFD,

$$\langle|\Phi|\rangle_* = \int_0^L |\Phi|\, u_*(x)\, dx \Big/ \int_0^L u_*(x)\, dx \qquad (19)$$

equals zero. The absolute value is taken because at the equilibrium due to zero flux boundary conditions always $\int_0^L \Phi u_* (x) \, dx = 0$ regardless of Φ deviating from zero. Our numerical results showed that in presence of ESS dispersal $\langle |\Phi| \rangle_* \neq 0$, but we tested the evolution of $\langle |\Phi| \rangle_*$ for the steady-state profiles in the iterations of ESS search algorithm. In all cases the closer the profile was to ESS case, the smaller $\langle |\Phi| \rangle_*$ was . Moreover, the greater $|b|$ was in our calculations, the smaller the observed ESS value of $\langle |\Phi| \rangle_*$ for the given habitat. We can conjecture that $\langle |\Phi| \rangle_*$ measures the closeness of the equilibrium distribution of individuals to IFD, and the closer it is, the greater is the species competitiveness in dispersal strategy. Fig. 8 shows the profiles of $\langle |\Phi| \rangle_* (b)$ for all our obtained ESS(b) dispersal strategies illustrated in Figs. 3 and 7. One can see an amazing correspondence between the skewness of $\langle |\Phi| \rangle_* (b)$ in Fig. 8a and asymmetry of mutual invasibility between FP and AD models in Fig. 7a. At the same time both $\langle |\Phi| \rangle_* (b)$ in Fig. 8b,c and mutual invasibility patterns in Fig. 7b,c are practically symmetric.

5. **Conclusions.** In this paper we derived a one-parameter family of diffusion-type dispersal models (4), where the parameter θ corresponds to a type of decision-making in the underlying random walk. Assuming that diffusion coefficient D depends on the fitness of individuals and using its two-parameter approximation (7), we attempted numerically to find an evolutionarily stable dispersal strategy in the resulting 3-parameter family of models generalizing the results of [6]. We developed a numerical algorithm for convergence to ESS dispersal. Our numerical results show that ESS corresponds to one of the two equations: 1) Fokker-Planck equation ($\theta = 0$) with diffusion coefficient (motility) having a minimum at the best parts of the domain and maximum at the worst ones and 2) AD equation ($\theta = 1$) with diffusion coefficient having minima at the worst parts of the habitat and maxima at the best ones. This finding agrees with the conjecture by P. Turchin [19] according to FP equation and the ideas of the ideal-free distribution [7]. Moreover, numerical results suggest that ESS dispersal strategy may correspond to population equilibrium with minimum mean absolute fitness (19).

Therefore, we can conclude that our results give evidence that Fokker-Planck equation and attractive dispersal equation may be a better alternative to modeling species dispersal than Fickian diffusion equation. Fitness-dependent diffusion coefficient allows to obtain population density distribution reasonably close to ideal-free distribution without minimizing diffusion coefficient, that is dispersal is working as a valuable adaptive mechanism.

Appendix.

Derivation of the diffusion equation for θ-random walk. Let us consider a one-dimensional random walk of a particle on a uniform 1D grid space $\{..., -2\delta, -\delta, 0, \delta, 2\delta, ...\}$ with constant step length δ and time interval τ. Let denote:
$v(x,t) := \text{Prob}(X(t) = x)$: probability of the particle being at location x at time t.
$p(x,s;y,t) := \text{Prob}(X(t) = y | X(s) = x)$: transition probability from location x at time s to y at time t.

From now on, we assume transition probabilities to be time-homogeneous, i.e. the probability of moving from x to y in a time interval τ is $p(x,t;y,t+\tau) = p(x;y)$.

Let us assume that there are functions $L(x)$, $R(x)$, $S(x)$, having at least two continuous derivatives, such that for some $0 \leq \theta \leq 1$,

$$p(x;x+\delta) = R(x+\theta\delta), \quad p(x;x-\delta) = L(x-\theta\delta)$$

and

$$p(x - \delta; x) = R(x - (1 - \theta)\delta), \quad p(x + \delta; x) = L(x + (1 - \theta)\delta).$$

Then the master equation in terms of the new transition probabilities is

$$\begin{aligned}
v(x, t + \tau) &= R(x - (1 - \theta)\delta)\, v(x - \delta, t) \\
&\quad + L(x + (1 - \theta)\delta)\, v(x + \delta, t) + S(x)\, v(x, t),
\end{aligned}$$

and we additionally have the conservation law

$$R(x + \theta\delta) + L(x - \theta\delta) + S(x) = 1.$$

Expanding both equations in Taylor series yields

$$\begin{aligned}
&v(x, t) + \tau \frac{\partial v}{\partial t} + O(\tau^2) \\
&= \left(v(x, t) - \delta \frac{\partial v}{\partial x} + \frac{\delta^2}{2} \frac{\partial^2 v}{\partial x^2} \right) \left(R(x) - \delta(1 - \theta) \frac{\partial R}{\partial x} + \frac{\delta^2}{2}(1 - \theta)^2 \frac{\partial^2 R}{\partial x^2} \right) \\
&\quad + \left(v(x, t) + \delta \frac{\partial v}{\partial x} + \frac{\delta^2}{2} \frac{\partial^2 v}{\partial x^2} \right) \left(L(x) + \delta(1 - \theta) \frac{\partial L}{\partial x} + \frac{\delta^2}{2}(1 - \theta)^2 \frac{\partial^2 L}{\partial x^2} \right) \\
&\quad + v(x, t) \left(1 - R(x) - \theta\delta \frac{\partial R}{\partial x} - \frac{\theta^2\delta^2}{2} \frac{\partial^2 R}{\partial x^2} - L(x) + \theta\delta \frac{\partial L}{\partial x} - \frac{\theta^2\delta^2}{2} \frac{\partial^2 L}{\partial x^2} \right) + O(\delta^3).
\end{aligned}$$

This simplifies to

$$\begin{aligned}
\frac{\partial v}{\partial t} + O(\tau) &= \frac{\partial}{\partial x} \left(\left(-\frac{\delta}{\tau}(R(x) - L(x)) \right.\right. \\
&\qquad\qquad \left. + (1 - 2\theta) \frac{\delta^2}{2\tau} \frac{\partial}{\partial x}(R(x) + L(x)) \right) v(x, t) \bigg) \\
&\qquad + \frac{\partial}{\partial x} \left(\frac{\delta^2}{2\tau}(R(x) + L(x)) \frac{\partial v}{\partial x} \right) + O\left(\frac{\delta^3}{\tau} \right).
\end{aligned}$$

Now, let $\tau \to 0$ and $\delta \to 0$, such that

$$\begin{aligned}
c(x) &= \lim_{\delta, \tau \to 0} \frac{\delta}{\tau}(R(x) - L(x)) \\
D(x) &= \lim_{\delta, \tau \to 0} \frac{\delta^2}{2\tau}(R(x) + L(x)).
\end{aligned}$$

The advection-diffusion equation is then

$$\frac{\partial v}{\partial t} = \frac{\partial}{\partial x} \left(-c(x)\, v(x, t) + (1 - 2\theta)D'(x)\, v(x, t) + D(x) \frac{\partial v}{\partial x} \right).$$

or, assuming $D \neq 0$,

$$\frac{\partial v}{\partial t} = \frac{\partial}{\partial x} \left(-c(x)\, v(x, t) + D^{2\theta}(x) \frac{\partial}{\partial x} \left(D^{1-2\theta}(x)v(x, t) \right) \right).$$

For $\theta = 0$, this is the Fokker-Planck equation or repulsive transition equation [14]. For $\theta = 1$, we obtain the attractive transition equation. If we set $\theta = \frac{1}{2}$, the middle term vanishes and we are left with Fickian diffusion or the neutral transition equation.

Analytical model for interface between good an bad habitat. Let us assume that to the left of the boundary $x_b = 0$ there is a good habitat with local population dynamics $f_L(u) = ru(1 - u^2)$ and dispersal coefficient $D_1 = 1$, and to the right of it $f_R(u) = -\alpha u$ and $D_2 = D$. Since within each subdomain the dispersal coefficient is constant, the system dynamics is described by

$$\begin{aligned} u_t &= u_{xx} + ru(1 - u^2), & x < x_b, \\ u_t &= Du_{xx} - \alpha u, & x > x_b. \end{aligned}$$

At $x = x_b$ we assume that the conditions (6) are satisfied.

We obtain the steady-state solution satisfying the conditions $u \to 1$ at $-\infty$ and $u \to 0$ at $+\infty$. To solve $u_{xx} + ru(1 - u^2) = 0$ we multiply it by u_x, then it can be integrated once,

$$\frac{1}{2}(u_x)^2 + \frac{r}{2}u^2 - \frac{r}{4}u^4 = C.$$

For $x \to -\infty$ we have $u_x \to 0$, $u \to 1$, so $C = r/4$. Therefore,

$$(u_x)^2 = \frac{r}{2}\left(1 - u^2\right)^2,$$

and since u decreases with x from 1 to zero, $u_x < 0$ and

$$u_x = -\sqrt{\frac{r}{2}}\left(1 - u^2\right),$$

with the solution

$$u_L(x) = \frac{Ae^{-\sqrt{2r}x} - 1}{Ae^{-\sqrt{2r}x} + 1} = 1 - \frac{2}{Ae^{-\sqrt{2r}x} + 1}, \qquad x < 0.$$

At the right hand side we have the equation $Du_{xx} - \alpha u = 0$ and the solution satisfying $u \to 0$ at $+\infty$ is

$$u_R(x) = B \exp\left(-\sqrt{\frac{\alpha}{D}}x\right), \qquad x > 0.$$

At the interface we have two conditions for matching u_L and u_R:

$$u_L(0) = D^{1-2\theta}u_R(0), \qquad u_{Lx}(0) = Du_{Rx}(0),$$

or the system of equations for A and B

$$\frac{A - 1}{A + 1} = D^{1-2\theta}B, \qquad -\frac{2\sqrt{2r}A}{(A + 1)^2} = -D\sqrt{\frac{\alpha}{D}}B.$$

Solving it we obtain

$$A = \sqrt{\frac{2rD^{1-4\theta}}{\alpha} + 1} + \sqrt{\frac{2rD^{1-4\theta}}{\alpha}}, \qquad B = D^{2\theta-1}\frac{A - 1}{A + 1}.$$

The results for $\alpha = 2$, $r = 4$, $\theta = 0, 0.5, 1$ and $D = 2$ and 0.5 are shown in Fig. 2.

REFERENCES

[1] P. A. Abrams and L. Ruokolainen, How does adaptive consumer movement affect population dynamics in consumer-resource metacommunities with homogeneous patches?, *J. Theor. Biol.*, **277** (2011), 99–110.

[2] D. G. Aronson, The role of diffusion in mathematical biology: Skellam revisited, in *Mathematics in Biology and Medicine* (eds. V. Capasso, E. Grosso, S.L. Paaveri-Fontana) Springer, Berlin, (1985), 2–6.

[3] J. E. Brittain and T. J. Eikeland, Invertebrate drift - a review, *Hydrobiologia,* **166** (1988), 77–93.

[4] R. S. Cantrell and C. Cosner, *Spatial Ecology Via Reaction-Diffusion Equations*, Wiley, The Atrium, Southern Gate, 2003.

[5] R. S. Cantrell, C. Cosner and Y. Lou, Approximating the ideal free distribution via reaction-diffusion-advection equations, *J. Differential Equations*, **245** (2008), 3687–3703.

[6] J. Dockery, V. Hutson, K. Mischaikow and M. Pernarowski, The evolution of slow dispersal rates: A reaction diffusion model, *J. Math. Biol.,* **37** (1998), 61–83.

[7] S. D. Fretwell and H. L. Lucas, On territorial behavior and other factors influencing habitat distribution in birds I. Theoretical development, *Acta Biotheoretica,* **19** (1969), 16–36.

[8] J. Hofbauer and K. Sigmund, *Evolutionary Games and Population Dynamics*, Cambridge Univ. Press, Cambridge, 1998.

[9] V. Křivan, R. Cressman and C. Schneider, The ideal free distribution: A review and synthesis of the game-theoretic perspective, *Theor. Population Biol.,* **73** (2008), 403–425.

[10] Y. Lou, Some Challenging Mathematical Problems in Evolution of Dispersal and Population Dynamics, in *Tutorials in Mathematical Biosciences IV* Lecture Notes in Mathematics Vol. 1922, Springer, Berlin Heidelberg (2008), 171–205.

[11] D. W. Morris, Adaptation and habitat selection in the eco-evolutionary process, *Proc. Roy. Soc. B*, **278** (2011), 2401–2411.

[12] D. W. Morris and P. Lundberg, *Pillars of Evolution*, Oxford Univ. Press, Oxford, 2011.

[13] L. Ni, A Perron type theorem on the principal eigenvalue of nonsymmetric elliptic operators, to appear in American Mathematical Monthly. Avalable online at URL: `http://math.ucsd.edu/~lni/academic/perron-1210-2.pdf`

[14] A. Okubo and S. Levin, *Diffusion and Ecological Problems*, Springer, NY, 2001.

[15] O. Ovaskainen and S. J. Cornell, Biased Movement at a Boundary and Conditional Occupancy Times for Diffusion Processes, *J. Appl. Prob.,* **40** (2003), 557–580.

[16] A. Potapov, Stochastic model of lake system invasion and its optimal control: neurodynamic programming as a solution method, *Nat. Res. Mod.,* **22** (2009), 257–288.

[17] R. Development Core Team, *R: A Language and Environment for Statistical Computing*, R Foundation for Statistical Computing, Vienna, Austria, 2007. ISBN 3-900051-07-0, `http://www.R-project.org`.

[18] H. E. Romeijn and R. L. Smith, Simulated annealing for constrained global optimization, *J. Global Optimization,* **5** (1994), 101–126.

[19] P. Turchin, *Quantitative Analysis of Movement*, Sinauer Assoc., Sunderland, MA., 1998.

E-mail address: `apotapov@ualberta.ca`
E-mail address: `ulrike.schlaegel@ualberta.ca`
E-mail address: `mark.lewis@ualberta.ca`